ELSEVIER

Diamond and Related Materials 11 (2002) 788–792

DIAMOND AND RELATED MATERIALS

www.elsevier.com/locate/diamond

# Study of carbon nanoemitters using $CO_2$–$CH_4$ gas mixtures in triode-type field emission arrays

C.F. Chen, C.L. Tsai*, C.L. Lin

*Department of Materials Science and Engineering, National Chiao Tung University, 1001 Ta-Hsueh Road, Hsinchu 30050, Taiwan, ROC*

---

**Abstract**

In this study, we used methane/carbon dioxide gas mixtures to deposit nanoemitters on the gate-structured metal–insulator–semiconductor (MIS) diodes. Due to the nanoemitters growing in a high carbon concentration gas source of $CH_4/CO_2$, the growth rate is better than conventional mixtures by using hydrocarbons diluted in hydrogen. Moreover, the bias also promotes the growth rate in the $CH_4/CO_2$ gas mixtures. In addition, selected area deposition (SAD) of emitters was successfully achieved by using the Pt layer as inhibitor in the bias assisted microwave plasma chemical vapor deposition (BAMPCVD). The field emission current and the current density of nanoemitters on field emission arrays (FEAs) are 154 μA and 490 mA $cm^{-2}$, respectively. This may be due to the following reasons: (I) short gate-emitter spacing; (II) small gate aperture; and (III) emitter with a sharp feature. © 2002 Elsevier Science B.V. All rights reserved.

*Keywords:* Field emission; CVD; SEM; Raman spectroscopy

---

## 1. Introduction

The emission of electrons from the surface of diamond and diamond-like carbon (DLC) films has attracted much attention due to its potential application in cold cathode devices. Diamond possesses negative electron affinity (NEA), in addition to remarkable characteristics such as large thermal conductivity and being chemically inert. Many studies have focused on fabricating diamond films [1] or diamond-clad silicon field emission arrays (FEAs) [2].

The most popular gas mixtures for the chemical vapor deposition (CVD) of diamond are hydrocarbon diluted in hydrogen. Therefore, hydrogen is a very high percentage in the gas mixtures and the diluted hydrocarbon gas is the only source of carbon. In this study, we used methane/carbon dioxide to deposit carbon nanoemitters in triode-type FEAs without hydrogen dilution. Furthermore, the selective area deposition (SAD) of nanoemitters by using a Pt layer as a nucleation inhibitor is also successfully completed in the CVD process.

## 2. Experiment

The fabrication process of the metal–insulator–semiconductor (MIS) diode and diamond-like deposition procedure have been previously presented [3]. First, we made the MIS diode structure by semiconductor process technology. Starting substrates were mirror-polish n-type, (100) oriented wafers with a resistivity of 4.5∼5.5 Ω $cm^{-1}$. After fabricating the MIS diode, specimens were put in the bias assisted microwave plasma chemical vapor deposition (BAMPCVD) system to deposit diamond with various deposition parameters. Fig. 1 shows the cross-section of the triode-type structure. The reactive gases used in deposition were the mixtures of $CH_4$–$CO_2$. The flow rates of $CH_4/CO_2$ and deposition time remained constant at 30/30 sccm and 15 min, respectively. While processing the deposition, the specimens were subjected to a negative bias voltage. Table 1 lists the experimental conditions.

Scanning electron microscopy (SEM) was used to observe the morphology of nanoemitters on FEAs,

---

*Corresponding author. Tel.: +886-9-3588-9532; fax: +886-6-261-6193.

*E-mail address:* lun@ms15.url.com.tw (C.L. Tsai), lun.mse89g@nctu.edu.tw (C.L. Tsai).

0925-9635/02/$ - see front matter © 2002 Elsevier Science B.V. All rights reserved.
PII: S0925-9635(01)00661-6

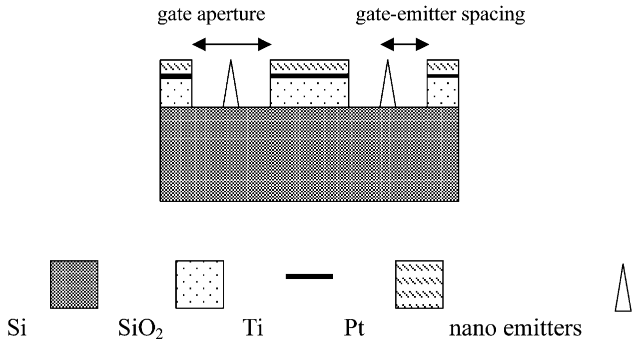

Fig. 1. The schematic cross-section of a triode device structure.

micro-Raman spectroscopy was used to identify the quality of emitters, and an $I$–$V$ measuring system to obtain their field emission characterization. The field emission properties of the FEAs were measured by using a triode technique. An anode plate, an ITO glass, was placed at 100 μm above the Pt-gate and was biased to +800 V. The anode current $(I_A)$ was then measured as a function of gate-to-cathode bias voltage in a vacuum of $1\times10^{-6}$ torr. The gate-to-cathode voltage $(V_{gc})$ was biased from 0 to 50 V. During testing, the device was in a common emitter configuration and both the anode and gate being positive potentials to turn the device on.

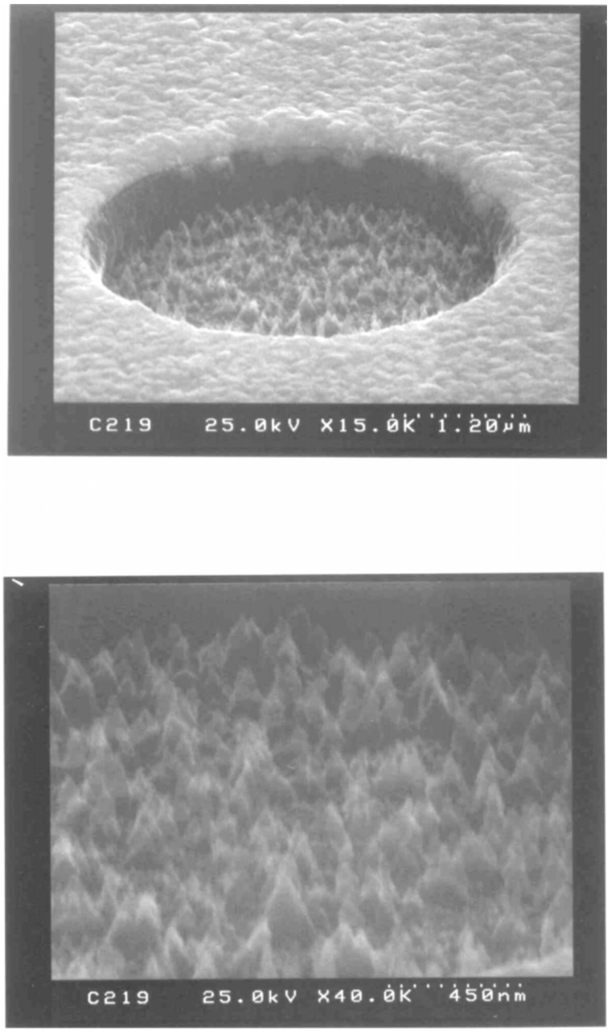

Fig. 2. SEM photograph of sample A growing under 120 V.

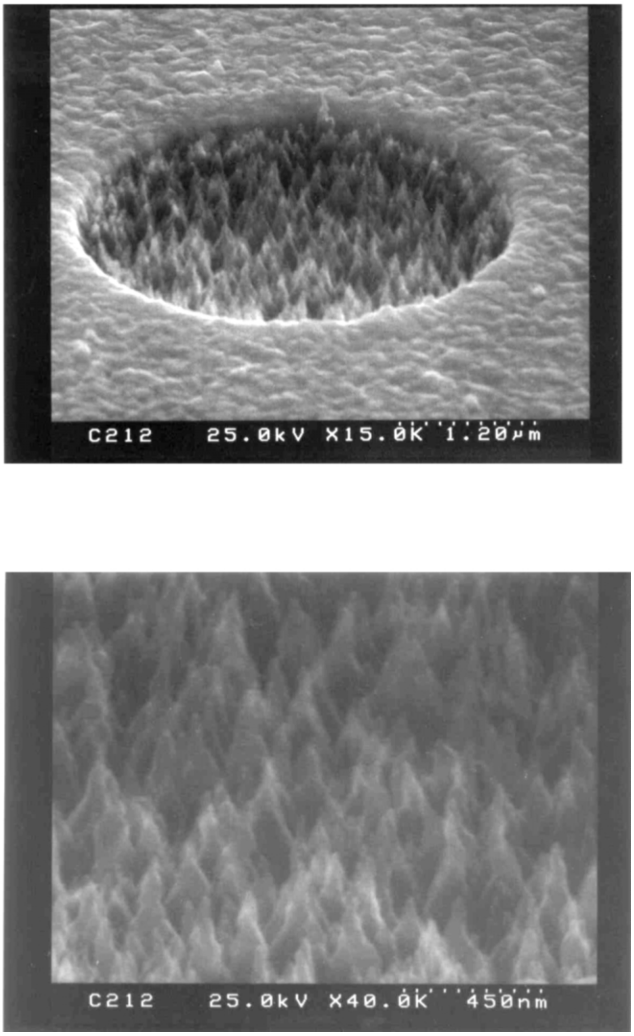

Fig. 3. SEM photograph of sample B growing under 130 V.

Table 1
Deposition conditions of nanoemitter

| Sample | Flow rate $CH_4/CO_2$ (sccm) | Negative bias (V) | Deposition time (min) |
|---|---|---|---|
| A | 30/30 | 120 | 15 |
| B | 30/30 | 130 | 15 |
| C | 30/30 | 150 | 15 |
| D | 30/30 | 180 | 15 |

Total pressure = 15 torr; microwave power = 300 W; Substrate temp. ≈750 °C.

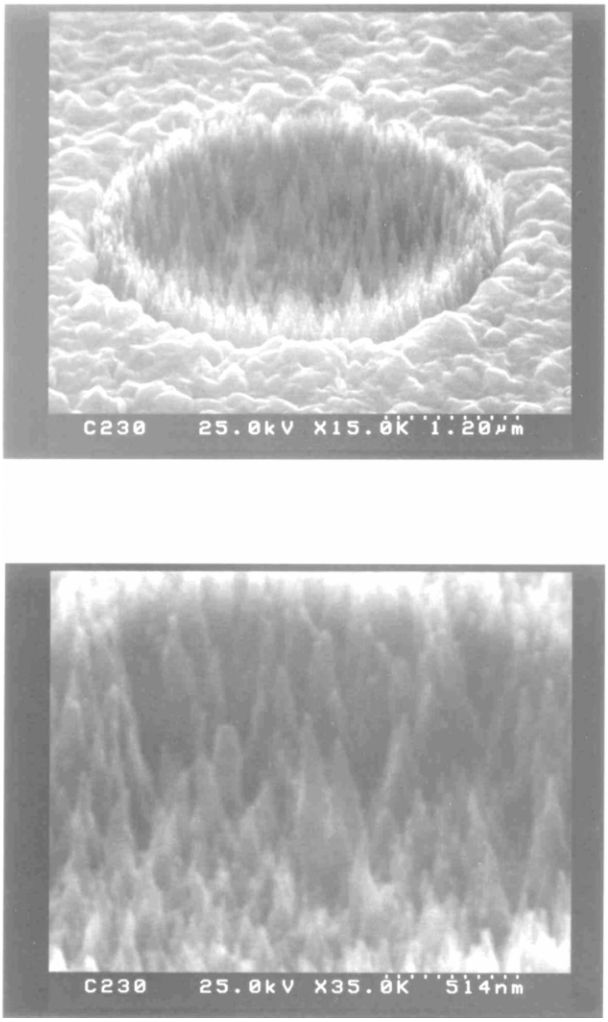

Fig. 4. SEM photograph of sample C growing under 150 V.

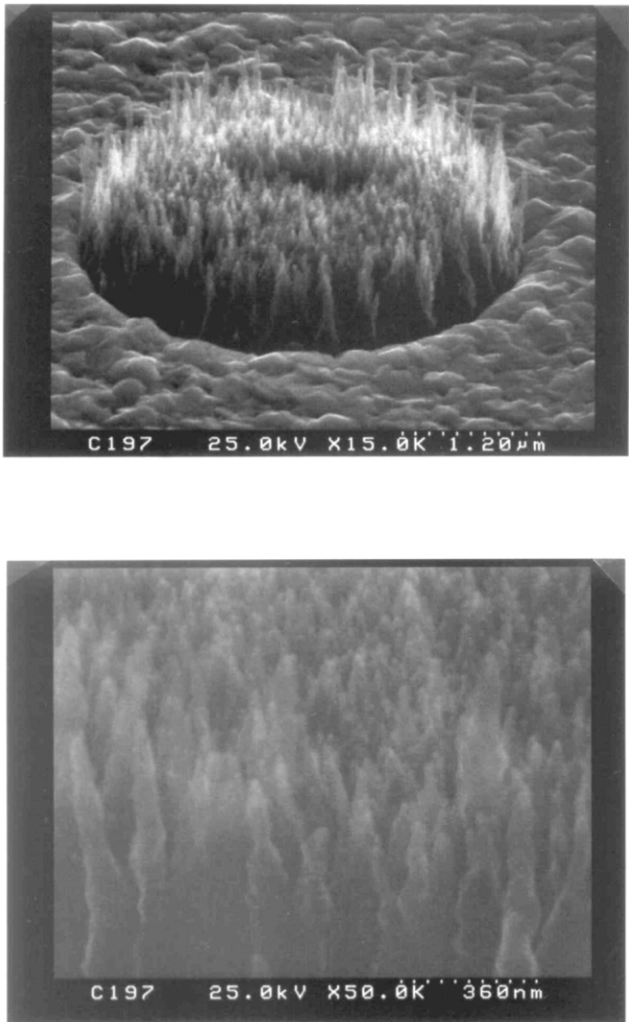

Fig. 5. SEM photograph of sample D growing under 180 V.

## 3. Results and discussion

Figs. 2–5 show SEM photographs of nanoemitters growing under different bias. Each picture is only one of the 50×50 circles on the FEAs. Every picture in the bottom side is an enlarged image of the top one. The width and the depth of the hole are 4 μm and 7000 Å, respectively. Under the bias below 130 V, there is only low density of tiny tips inside the hole. Fig. 2 shows a SEM photograph of the nanoemitters growing under 120 V. Once we increased the deposition time, which is over 15 min, not only inside the hole but also on the Pt-gate were carbon materials. Indeed, the carbon materials may replace the Pt to form the carbon-gated FEAs. In the worst case scenario, this phenomenon will taint the *I–V* measurement because the field emission current maybe be inexact because of the influence from both the nanoemitters and carbon-gated surface. Figs. 4 and 5 display that higher bias drastically enhances the growth

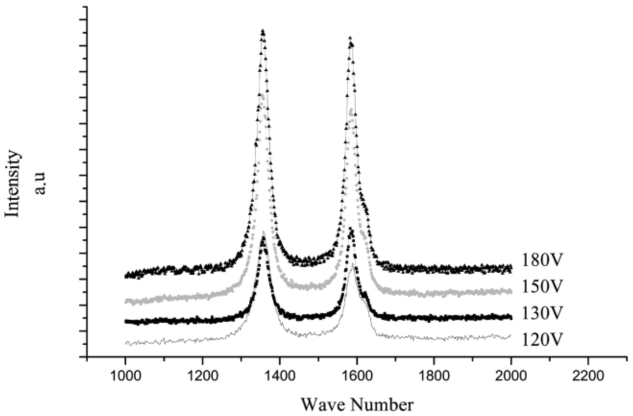

Fig. 6. Raman spectra of nanoemitters growing under different applied bias.

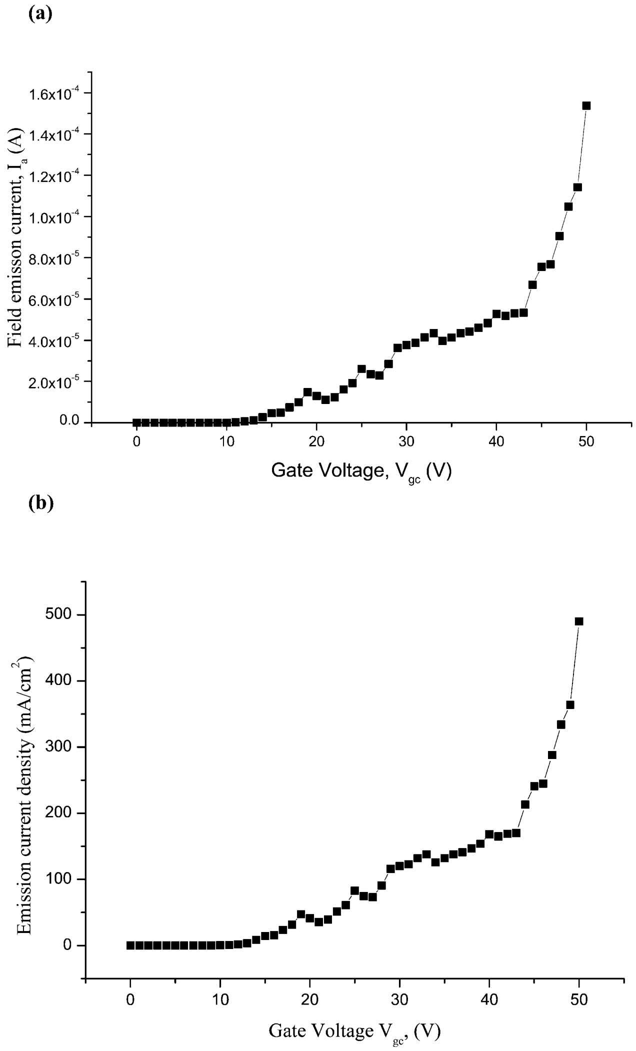

Fig. 7. (a) The emission current ($I_a$) vs. the gate voltage ($V_{gc}$) and (b) the emission current density ($J_e$) of nanoemitters growing under 130 V on FEAs.

rate of nanoemitters. However, this leads the triode-type device to a diode structure because of the emitters exceeding the height of the hole.

Examining Figs. 2–5, we get the following results. (I) The applied bias can enhance the growth rate of nanoemitters with $CH_4/CO_2$ gas mixtures in CVD process. Moreover, the higher bias is applied, the higher growth rate is obtained. The bias effect is also valid for the hydrocarbon diluted in hydrogen [4]. (II) The growth rate of $CH_4/CO_2$ gas mixtures is better than the conventional gas $CH_4/H_2$ [5]. This is due to the nanoemitters growing in a high carbon concentration gas source of $CH_4/CO_2$. (III) In addition, the deposition under high bias will cause higher density, larger and sharper nanoemitters. Thus, emitters with sharp features have small radius curvature and high aspect ratio. (IV) All the emitters directly grow upward under bias condition.

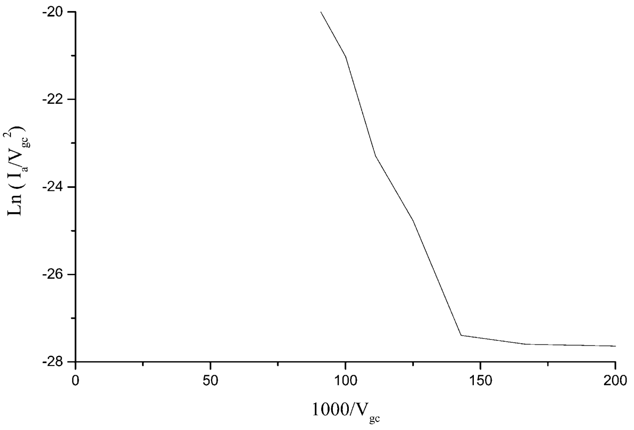

Fig. 8. The *F–N* plot of nanoemitters growing under 130 V on FEAs.

The region for diamond growth is indicated in the C–H–O diagram presented by Bachmann et al. [6]. The parameter range for diamond deposition from $CH_4/CO_2$ is narrower than the $CH_4/H_2$. The molar ratio of $CH_4/CO_2 = 1.08 \sim 1.63$ is needed for diamond growth. In terms of the ratio of C/O, the range is from 1.04 to $\sim 1.31$. When the ratio is out of this range, the graphite is found on the deposit. In other words, the growth conditions are very restrictive. Nevertheless, due to the difference of various deposition conditions such as microwave power, pressure and substrates, etc., the results maybe change. In this study, the volume ratio of $CH_4/CO_2 = 1$ is used.

Fig. 6 shows Raman spectra of emitters growing under applied various bias. We find there is no obvious difference among these spectra. All of them have two sharp peaks located at approximately 1355 $cm^{-1}$ and 1582 $cm^{-1}$, respectively. These imply that the nanoemitters are characteristic of microcrystalline graphite. The Raman spectra of amorphous carbon can be decomposed into two features located approximately at 1550 $cm^{-1}$ (corresponding to the G-line associated with the optically allowed $E_{2g}$ zone center mode of crystalline graphite) and 1350 $cm^{-1}$ (roughly corresponding to the D-line associated with disorder-allowed zone-edge modes of graphite). The positions, widths, and relative intensities of these two peaks are found to vary systematically with deposition conditions and emitters' properties [7,8]. The intensity of these two peaks is the same. This indicates that there is much amorphous carbon in the samples.

Fig. 7 displays the electron-emitting characteristic of the nanoemitters growing under 130 V on FEAs. If the applied bias is above 130 V, the emitters will grow over the hole. This indicates that the emitters exceed the height of Pt-gate. Under this condition, the device becomes diode structure instead of triode-type one. The field emission current ($I_a$) of nanoemitters from all of the holes on FEAs is approximately 154 μA (at gate-to-cathode voltage, $V_{gc}=50$ V). A display requires at least 1 mA cm$^{-2}$ to excite the phosphorus pixel. Thus the emission current density ($J_e$) obtained from nanoemitters on all holes is approximately 490 mA cm$^{-2}$. Therefore, the higher emission current density of the nanoemitters on FEAs is due to the following reasons: (I) short gate-emitter spacing; (II) small gate aperture; and (III) emitters possessing sharp feature with small radius [9,10]. It has been shown that the tip radius of curvature and the gate aperture influence the field enhancement factor β most significantly; i.e. β increases rapidly as tip radius and gate aperture decrease [11–13].

The threshold voltage ($V_{th}$) is defined as the intersection of the *F–N* plots shown in Fig. 8 with the abscissa. The threshold voltage ($V_{th}$) is approximately 13 V for the nanoemitters. Due to the smaller gate aperture; diameter and shallower gate structure, a field emission can be triggered at a lower threshold voltage. However, there is a saturated current at $V_{gc}=50$ V for nanoemitters on FEAs. This phenomenon is caused by the fact that the dielectric layer ($SiO_2$) in the developed pattern may be broken under high applied voltage, which will create a leakage current.

## 4. Conclusions

In this study, we successfully fabricated the triode-type FEAs for decreasing the turn-on voltage and increasing the emission current. Results are summarized as follows.

1. First, we successfully completed the selective area deposition (SAD) of nanoemitters by using a Pt-layer as a nucleation inhibitor in the BAMPCVD process.
2. Due to the nanoemitters growing in a high carbon concentration gas source of $CH_4/CO_2$, the growth rate is better than with conventional mixtures by using hydrocarbons diluted in hydrogen ($CH_4/H_2$).
3. The higher bias is applied, the higher the growth rate obtained in the $CH_4/CO_2$ gas mixtures.
4. The emission current and current density for the nanoemitters on FEAs are 154 μA and 490 mA cm$^{-2}$, respectively. The turn-on voltage is approximately 13 V. This is due to the effect of: (I) small gate aperture; (II) the short gate-emitter spacing; and (III) emitters possessing sharp features with small radius.

## References

[1] A. Watanabe, M. Deguchi, M. Kitabatake, Diamond Relat. Mater. 10 (2001) 818.
[2] N.J. She, A Study of Application and Characterization of Diamond Thin Films on Field Emitter Arrays, Master's Thesis, Chiao Tung University, 1996.
[3] C.F. Chen, H.C. Wang, H.C. Hsieh, Jpn. J. Appl. Phys. 39 (2000) 1880–1884.
[4] S. Yugo, T. Kanai, T. Kimura, T. Muto, Appl. Phys. Lett. 58 (1991) 1036.
[5] C.-F. Chen, H.-c. Hsieh, Diamond Relat. Mater 9 (2000) 1257.
[6] P.K. Bachmann, D. Leers, H. Lydtin, Diamond Relat. Mater. 1 (1991) 1.
[7] M.A. Tamor, W.C. Vassell, J. Appl. Phys 76 (6) (1996) 3823.
[8] J. Wagner, M. Ramsteiner, Ch. Wild, P. Koidl, Phys. Rev. B 40 (1989) 1817.
[9] J.M. Kim, Process Technology and Characterization for Field Emission Devices, Michigan UMI, 1992, p. 10.
[10] D. Temple, Mater. Sci. Eng. R 24 (1999) 191.
[11] R.B. Marcus, K.K. Chin, Y. Yuan, H. Wang, W.N. Carr, IEEE Trans. Electron Dev. 37 (1990) 1545.
[12] J.H. Kang, J.W. Cho, J.W. Kim, J.M. Kim, J.Vac. Sci. Technol. B14 (1996) 1924.
[13] E.G. Zaidman, K.L. Jensen, M.A. Kodis, J. Vac. Sci. Technol. B 14 (1996) 1994.